

Investigation of the Origin of the Empirical Relationship between Refractive Index and Density on the Basis of First Principles Calculations for the Refractive Indices of Various TiO₂ Phases

Xavier Rocquefelte,[†] Fabrice Goubin,[†] Hyun-Joo Koo,[‡] Myung-Hwan Whangbo,^{*,†} and Stéphane Jobic^{*,†}

Laboratoire de Chimie des Solides, Institut des Matériaux Jean Rouxel, 2 rue de la Houssinière, BP 32229, 44322 Nantes Cedex 03, France, and Department of Chemistry, North Carolina State University, Raleigh, North Carolina 27695-8204

Received December 2, 2003

On the basis of first principles electronic structure calculations, we determined the dielectric functions, the refractive indices, and the extinction coefficients of the seven different phases of TiO₂ and then examined why the refractive index is related to the density by the empirical Gladstone–Dale equation. The zero frequency limit of the refractive index, n_0 , is found to be a good approximation for the refractive index n determined around 2 eV. Our study indicates that the major factor influencing n in a series of closely related systems is the structure compactness. This finding suggests a way of preparing new UV absorbers with low refractive index.

Introduction

Light-absorbing minerals have received much attention during the past decade owing to their potential industrial interest as inorganic pigments and/or UV blockers. The development of new colored inorganic materials is motivated by the urgent need to limit the use of heavy-elements-based industrial pigments hazardous to health and environment,^{1,2} and that of new inorganic UV absorbers by the increasing need to block the costly deterioration of polymer matrixes (plastic, wood, etc.) and the alteration of biological tissues exposed to UV radiations.^{3–7}

The development of new pigments and particulate-based

sunscreens requires the knowledge of the optical properties of inorganic materials, namely, the refractive index n and the extinction coefficient k . These two quantities, which depend on the wavelength λ of the impinging light, form the complex refractive index $N(\lambda) = n(\lambda) + ik(\lambda)$. The opacity (i.e., the light scattering power) and the color strength (i.e., the light-absorbing capacity) of inorganic materials depend on n and k , respectively. Alternatively, the interaction of light with materials can be discussed in terms of the complex dielectric function $\epsilon(\lambda) = \epsilon_1(\lambda) + i\epsilon_2(\lambda)$, which describes the linear response of the electronic structure of an insulating material to the electrical field of the incident radiation with a wavelength λ . The real part $\epsilon_1(\lambda)$ is related to the electronic polarizability of the material, and the imaginary part $\epsilon_2(\lambda)$ is associated with the electronic absorption of the material. n and k are related to ϵ_1 and ϵ_2 as follows:

$$n = \frac{(\epsilon_1 + (\epsilon_1^2 + \epsilon_2^2)^{0.5})^{0.5}}{\sqrt{2}} \quad k = \frac{(-\epsilon_1 + (\epsilon_1^2 + \epsilon_2^2)^{0.5})^{0.5}}{\sqrt{2}} \quad (1)$$

$$\epsilon_1 = n^2 - k^2 \quad \epsilon_2 = 2nk \quad (2)$$

n and k are isotropic for a cubic system. They are anisotropic

* To whom correspondence should be addressed. E-mail: jobic@cnrs-imn.fr (S.J.); mike_whangbo@ncsu.edu (M.-H.W.).

[†] Institut des Matériaux Jean Rouxel.

[‡] North Carolina State University.

- (1) Jansen, M.; Letschert, H. P. *Nature* **2000**, *404*, 980.
- (2) *European Economic Community Guideline*, no. 91/338/EWG, 1991.
- (3) Pathak, M. A. Photoprotection Against Harmful Effects of Solar UVB and UVA Radiation: An Update. In *Sunscreens: Development, Evaluation, and Regulatory Aspects*; Lowe, N. J., Shaath, N. A., Pathak, M. A., Eds.; Marcel Dekker Inc.: New York, 1997.
- (4) Rabek, J. F. *Photodegradation of Polymers: Physical Characteristics and Applications*; Springer-Verlag: Berlin, 1996.
- (5) Deglise, X.; Merlin, A. Comportement Photochimique du Bois non Traité. In *Durabilité des Bois et Problèmes Associés*; Dirol, D., Deglise, X., Eds.; Hermès Science Publication: 2001.
- (6) Anderson, M. W.; Hewitt, J. P.; Spruce, S. R. Broad-Spectrum Physical Sunscreens: Titanium Dioxide and Zinc Oxide. In *Sunscreens: Development, Evaluation, and Regulatory Aspects*; Lowe, N. J., Shaath, N. A., Pathak, M. A., Eds.; Marcel Dekker Inc.: New York, 1997.

- (7) Fairhurst, D.; Mitchnick, M. A. Particulate Sun Blocks: General Principles. In *Sunscreens: Development, Evaluation, and Regulatory Aspects*; Lowe, N. J., Shaath, N. A., Pathak, M. A., Eds.; Marcel Dekker Inc.: New York, 1997.

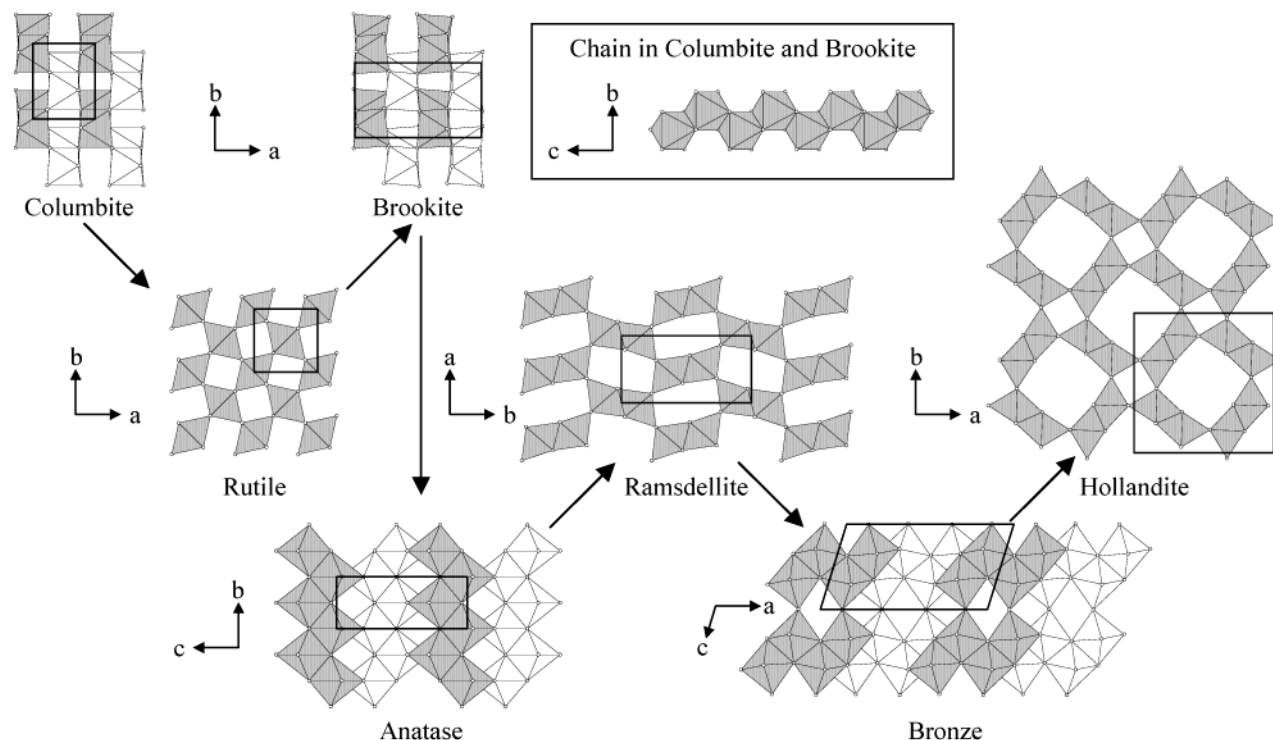


Figure 1. Schematic polyhedral representations of the seven TiO_2 phases. For more detailed descriptions, see Hyde and Anderson.¹⁹

and characterized by two sets of values for uniaxial compounds (e.g., tetragonal, rhombohedral, and hexagonal systems) and by three sets of values for biaxial compounds (e.g., triclinic, monoclinic, and orthorhombic systems).

Contrary to some intuitive ideas, the main difference between pigments and UV absorbers does not lie in the position of the absorption threshold but rather in the value of the refractive index. UV absorbers need to minimize light scattering in the visible region (low n value), while the opposite is required for pigments (high n value). According to this consideration, TiO_2 is a white pigment, although a transparent grade, obtained by making particles extremely small, is widely used for UV blocker applications.⁶

For a large number of minerals, it has been well established that the refractive index is related to the mass density ρ_m (i.e., the mass of the formula unit divided by the volume/formula unit) by an empirical relationship such as the Gladstone–Dale (GD) equation.⁸ Initially, the density d and the refractive index n of organic liquids were found to obey the relationship $(n - 1)/d = \text{constant}$ by Gladstone and Dale. Later, this formula has been found to work very well for minerals within about 5% precision.^{9,10} Since the refractive index of a compound is a property associated with its electronic structure, it is natural to think that the influence of chemical modifications (substitution, structure changes, etc.) on the optical properties would be complex to understand. Thus, one may wonder why the refractive indices for a series of related compounds should be correlated with their mass densities ρ_m .

Table 1. Structural Details of Seven TiO_2 Phases

	space group	no. of sharing octahedral		
		corners	edges	vol/formula unit (\AA^3)
columbite ²⁰	$Pbcn$	8	2	30.58
rutile ²¹	$P4_2/mnm$	8	2	31.22
brookite ²²	$Pbca$	6	3	32.17
anatase ²³	$I4_1/amd$	4	4	34.06
ramsdellite ²⁴	$Pbnm$	4	4	34.30
bronze ²⁵	$C2/m$	4	4.5 ^a	35.53
hollandite ²⁶	$I4/m$	4	4	38.26

^a This is an average value due to two different titanium environments.

Thus, it is important to examine why the empirical relationship such as the GD equation works reasonably well. In this work we probe this question by calculating the dielectric functions and refractive indices of the seven different phases of TiO_2 on the basis of first principles electronic band structure calculations. These systems are ideal for our study, because they exhibit a wide variation in their ρ_m (Table 1 and Figure 1) despite the fact that their building blocks, TiO_6 octahedra, are the same. So far, experimental refractive indices are known only for three TiO_2 phases. In the following we show that these compounds follow the empirical GD equation reasonably well and then probe why this empirical relationship works.

One-Electron Optical Properties of Solids

The one-electron model used to calculate the optical properties of extended solids has been extensively described by Bassani et al.¹¹ and by Lynch.¹² If the wavelength of light is long compared with the interatomic distances, then the

(8) Gladstone, J. H.; Dale, T. P. *Philos. Trans. R. Soc. London* **1863**, 153, 317.

(9) Jaffe, H. W. *Am. Mineral.* **1956**, 41, 757.

(10) Mandarino, J. A. *Can. Mineral.* **1981**, 19, 441.

(11) Bassani, F.; Pastori Parravicini, G.; Ballinger, R. A. *Electronic States and Optical Transitions in Solids*; Pamplin, B. R., Ed.; Pergamon Press: London, 1975.

transition probability W_{if} per unit time between a filled orbital $\varphi_i(\mathbf{k}, \mathbf{r})$ and an empty orbital $\varphi_f(\mathbf{k}, \mathbf{r})$ of the one-electron state is written as

$$W_{if} = \frac{2\pi(eA_0)^2}{\hbar} |\mathbf{eM}_{if}(\mathbf{k})|^2 \delta(E_f(\mathbf{k}) - E_i(\mathbf{k}) - \hbar\omega) \quad (3)$$

where $E_i(\mathbf{k})$ and $E_f(\mathbf{k})$ are the energies of the initial and the final states, respectively, A_0 is the magnitude of the electric field of the light, and the transition moment $\mathbf{M}_{if}(\mathbf{k})$ is given by

$$\mathbf{M}_{if}(\mathbf{k}) = \int \varphi_i^*(\mathbf{k}, \mathbf{r})(-i\hbar\nabla)\varphi_f(\mathbf{k}, \mathbf{r}) \, d\mathbf{r} \quad (4)$$

By summation over \mathbf{k} , over the spin variable, and over the band indices i (occupied) and f (empty), the probability $W(\omega)$ that the incident light loses the energy $\hbar\omega$ to induce an interband excitation within a unit volume per unit time is obtained as

$$W(\omega) = \frac{2\pi(eA_0)^2}{\hbar} \sum_{i,f} \int_{\text{BZ}} \frac{2d\mathbf{k}}{(2\pi)^3} |\mathbf{eM}_{if}(\mathbf{k})|^2 \delta(E_f(\mathbf{k}) - E_i(\mathbf{k}) - \hbar\omega) \quad (5)$$

where the integration over \mathbf{k} extends over the first Brillouin zone and the factor 2 arises from the integration of the spin variables. The imaginary part ϵ_2 of the dielectric function is related to $W(\omega)$ as

$$\epsilon_2(\omega) = \left(\frac{2\pi c^2}{A_0^2} \right) \frac{W(\omega)}{\omega^2} \quad (6)$$

This formula, valid for vertical electronic transitions (i.e., $\Delta k = 0$), connects straightforwardly the band structure with the optical properties. The real and imaginary parts of the dielectric function are linked by Kramers–Kronig relations,¹³ so that

$$\epsilon_1(\omega) = 1 + \frac{2}{\pi} P \int_0^{+\infty} \frac{\omega' \epsilon_2(\omega')}{\omega'^2 - \omega^2} d\omega' \quad (7)$$

where P indicates the principal value, i.e.,

$$P = \lim_{a \rightarrow 0} \int_{-\infty}^{\omega-a} \frac{\epsilon(\omega')}{\omega' - \omega} d\omega' + \lim_{a \rightarrow 0} \int_{\omega+a}^{+\infty} \frac{\epsilon(\omega')}{\omega' - \omega} d\omega' \quad (8)$$

Thus, once ϵ_1 and ϵ_2 are determined from electronic band structures, the optical constants n and k can be calculated according to eq 1. In particular, the zero frequency limit of $n(\lambda)$, i.e., n_0 , is obtained by integrating the extinction coefficient $k(\omega)$ weighted with the inverse of the excitation energy, $1/\omega$, namely

$$n_0 = 1 + \frac{2}{\pi} \int_0^{+\infty} \frac{k(\omega)}{\omega} d\omega \quad (9)$$

Computational Details

Our calculations were based on the density functional theory (DFT). The Perdew–Burke–Ernzerhof generalized gradient approximation¹⁴ (GGA) was used for the exchange and correlation correction. The density of states and the complex part of the dielectric function were deduced from a self-consistent calculation, using the full-potential linearized augmented plane wave (FP-LAPW) method, as embodied in the WIEN2k code.¹⁵ The maximum l value in the expansion of the basis set inside atomic sphere was 12 for the computation of muffin-tin matrix elements and 4 for that of the non-muffin-tin matrix elements. The convergence of basis set was controlled by a cutoff parameter $R_{\text{mt}} \times K_{\text{max}} = 8$, where R_{mt} is the smallest atomic sphere radius in the unit cell and K_{max} is the magnitude of the largest \mathbf{k} vector. The self-consistency were carried out on a 300 k -points mesh in the full Brillouin zone, with the following radii $R_{\text{mt}}(\text{Ti}) = 2.0$ au and $R_{\text{mt}}(\text{O}) = 1.4$ au and $\text{GMAX} = 14$ bohr⁻¹.

The imaginary part of the dielectric tensor was calculated using the one-electron orbitals and energies obtained from solving the Kohn–Sham equations. Under the rigid band and Koopmans' approximations and in the limit of linear optics^{11,12} and of the visible–ultraviolet region, the matrix element of the dielectric tensor has the imaginary part given by eq. 6. ϵ_2 was systematically calculated for $\hbar\omega$ up to 40 eV. A Kramers–Kronig transformation was employed to obtain the real part $\epsilon_1(\omega)$ from $\epsilon_2(\omega)$ using a Lorentzian broadening of 0.05 eV. The isotropic dielectric function was calculated by averaging the diagonal matrix elements, i.e., $\epsilon_{\text{iso}} = (\epsilon_{xx} + \epsilon_{yy} + \epsilon_{zz})/3$, and used to determine the average n and k values. The zero frequency limit of $n(\lambda)$, n_0 , can be regarded in a crude approximation as the refractive index usually given in the visible range at about 2 eV (i.e., at the yellow sodium doublet emission). This approximation is reasonable because the absorption thresholds of the different TiO₂ phases associated with O²⁻ → Ti⁴⁺ charge transfer excitations are high enough in energy. For dielectric tensor calculations, the BZ integration was carried out using 2000 k -points. Finer k -point grids did not modify the values of the dielectric tensors. No scissors operator was introduced in this study; that is, the bands lying above the valence bands were not shifted.

Results

The structures of the seven TiO₂ phases studied in our work are shown in Figure 1. The building blocks of all these phases are distorted TiO₆ octahedra with similar Ti–O bonds in strength. The compactness of the structure, which is directly related to the volume and the density, depends on how the TiO₆ octahedra are condensed and on whether the condensed structures have void cavities (Table 1 and Figure 1). The volume/formula unit increases in the order hollandite ($\rho_m = 3.47$ g/cm³) < bronze ($\rho_m = 3.73$ g/cm³) < ramsdellite ($\rho_m = 3.87$ g/cm³) < anatase ($\rho_m = 3.89$ g/cm³) < brookite ($\rho_m = 4.12$ g/cm³) < rutile ($\rho_m = 4.25$ g/cm³) < columbite ($\rho_m = 4.34$ g/cm³).

- (12) Lynch, W. D. Interband Absorption-Mechanisms and Interpretations. In *Handbook of Optical Constants of Solids*; Palik, E. D., Ed.; Academic Press: New York, 1985.
- (13) Smith, D. Y. Dispersion Theory, Sum Rules and their Application to the Analysis of Optical Data. In *Handbook of Optical Constants of Solids*; Palick, E. D., Ed.; Academic Press: New York, 1985.

- (14) Perdew, J. P.; Burke, S.; Ernzerhof, M. *Phys. Rev. Lett.* **1996**, *77*, 3865.
- (15) Blaha, P.; Schwarz, K.; Madsen, G. K. H.; Kvasnicka, D.; Luitz, J. WIEN2k: An Augmented Plane Wave + Local Orbitals Program for Calculating Crystal Properties, revised edition June 2002; Techn. Universität Wien, A-1060 Wien, Austria, 2001; ISBN 3-9501031-1-2.

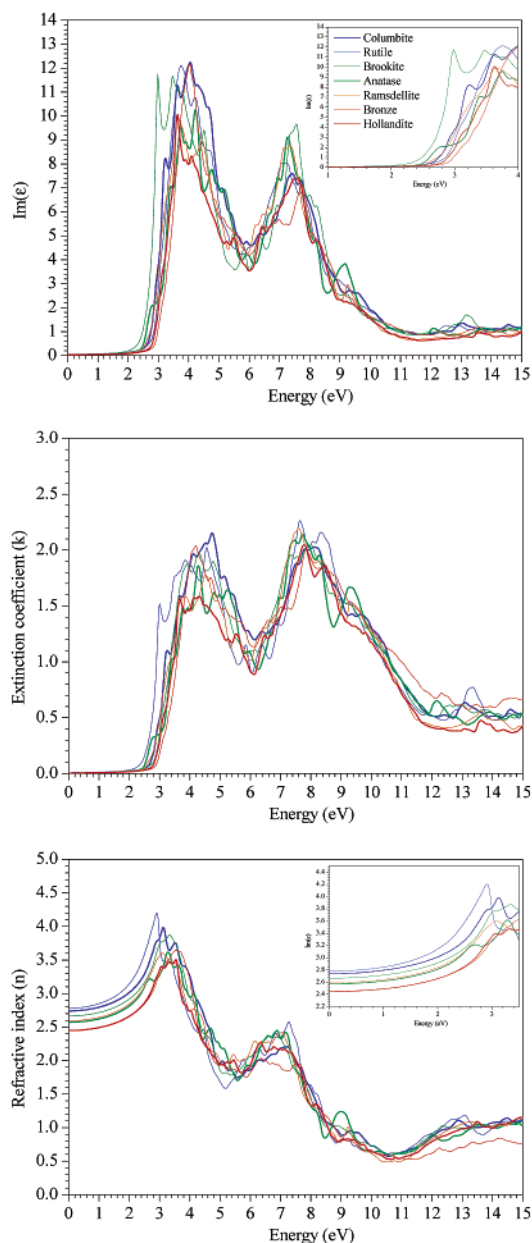


Figure 2. Calculated optical properties of seven TiO₂ phases: the isotropic imaginary part ϵ_2 of the dielectric function, the extinction coefficient k , and the refractive index n .

For the seven TiO₂ phases, Figure 2 displays the variation of $\epsilon_2(\omega)$, $k(\omega)$, and $n(\omega)$ as a function of the energy of the incident radiation $E = \hbar\omega$. To check the accuracy of our calculations, we compare the calculated refractive indices with the experimental data available for the rutile, brookite, and anatase phases.¹⁶ As summarized in Table 2, the n_0 values deduced from our DFT calculations agree reasonably well with the available experimental values n_{exp} and satisfactorily follow the GD equation $n_{\text{GD}} = 1 + 0.4\rho_m$ (Table 2 and Figure 3). It is well-known that DFT calculations underestimate the optical gap. The discrepancies between n_0 and n_{GD} are most likely due to errors in the optical gap inherent in DFT calculations.¹⁷ Moreover, the n_0 value should

(16) Lide, D. R. *Handbook of Chemistry and Physics*; CRC: Boca Raton, FL, 2003.

(17) Sham, L. J.; Schlüter, M. *Phys. Rev. Lett.* **1983**, *51*, 1888.

Table 2. Refractive Indices of TiO₂ Phases Obtained by Experiment (n_{exp}), the Gladstone–Dale Equation (n_{GD}), and DFT Calculations (n_0)

	n_{exp}	n_{GD}	n_0
columbite		2.73	2.74
rutile	2.71	2.70	2.78
brookite	2.64	2.65	2.66
anatase	2.53	2.56	2.57
ramsdellite		2.55	2.59
bronze		2.49	2.45
hollandite		2.39	2.45

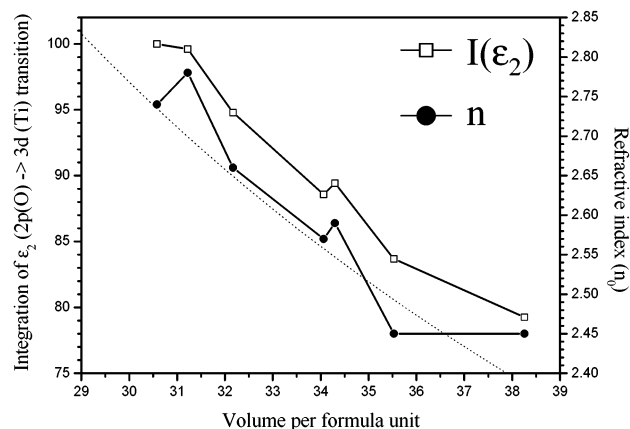


Figure 3. Calculated transition intensities $I(\epsilon_2)$ (normalized to 100 for the columbite phase) and refractive indices n_0 of seven TiO₂ phases versus volume/formula unit. The dotted line corresponds to the refractive indices obtained from the Gladstone–Dale equation.

be viewed only as an estimate for the refractive index reported in the literature.

Discussion

The electronic excitations determining the optical properties are associated with the valence electrons. Thus, one might consider the valence electron density (i.e., the number of valence electrons per formula unit divided by the volume per formula unit), ρ_e , as the more meaningful physical parameter to describe the refractive index. Since ρ_e is linearly related to ρ_m , it is understandable why the GD equation can describe the refractive indices of minerals.

We now examine why the refractive index is rather well described by the electron density ρ_e on the basis of eqs 1 and 9. It should be noted from eq 2 shows that $k(\omega)$ becomes nonzero only if $\epsilon_2(\omega)$ is nonzero. When a system has a smaller optical gap E_g , $k(\omega)$ becomes nonzero at a smaller ω thereby increasing the contribution of the $k(\omega)/\omega$ value in eq 9. Consequently the variation of the optical gap E_g can have a significant influence on the n_0 value. Similarly, for a given absorption threshold located in UV, a decrease in the extinction coefficient will induce a decrease of n_0 . For the TiO₂ phases, the calculated optical gaps (determined from the $\epsilon_2(E)$ curve as the intersection of the tangent of the absorption threshold with the energy axis) do not exhibit any trend as a function of the volume/formula unit (2.64, 2.2, 2.8, 2.44, 2.5, 2.85, and 2.8 eV for the columbite, the rutile, the brookite, the anatase, the ramsdellite, the bronze, and the hollandite forms of TiO₂, respectively). Figure 3 summarizes the integrated value of ϵ_2 , namely, $I(\epsilon_2)$,

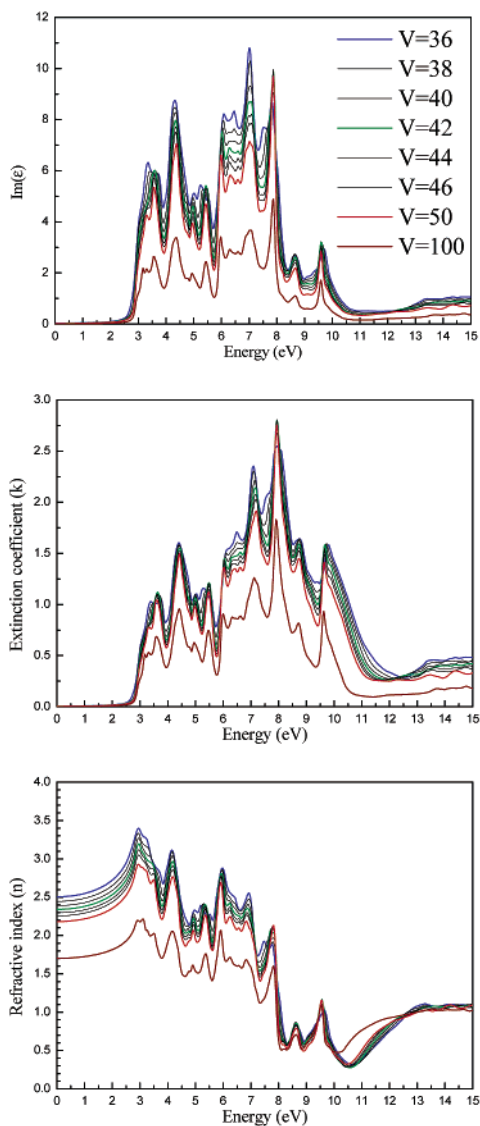


Figure 4. Calculated optical properties of a hypothetical CdI₂ structure¹⁸ of TiO₂ as a function of anisotropic change in the volume/formula unit (the volume was increased by increasing only the interlayer spacing): the isotropic imaginary part ϵ_2 of the dielectric function, the extinction coefficient k , and the refractive index n .

$$I(\epsilon_2) = \int_0^{+\infty} \epsilon_2(\omega) d\omega \quad (10)$$

and the refractive indices n_0 of the seven TiO₂ phases as a function of the volume/formula unit. Clearly, $I(\epsilon_2)$ and n_0 decrease with increasing volume/formula unit but do not appear to depend on the calculated optical gap. For all the seven TiO₂ phases, the product of $I(\epsilon_2)$ and the volume/formula unit V is almost constant, i.e., $I(\epsilon_2)V = 99.5 \pm 1.4$ (the calculation of $I(\epsilon_2)V$ was carried out by normalizing the intensity and the volume the columbite phase at 100 and 1, respectively). Namely, the integrated capability/unit formula to absorb light is the same, so that the major factor differentiating the refractive indices of the different TiO₂ phases is their volume/formula unit only.

To explore implications of the above observation, we examined the volume dependence of $I(\epsilon_2)$ and n using a hypothetical CdI₂-type structure of TiO₂, which consists of TiO₂ layers made up of TiO₆ octahedra. The volume/formula

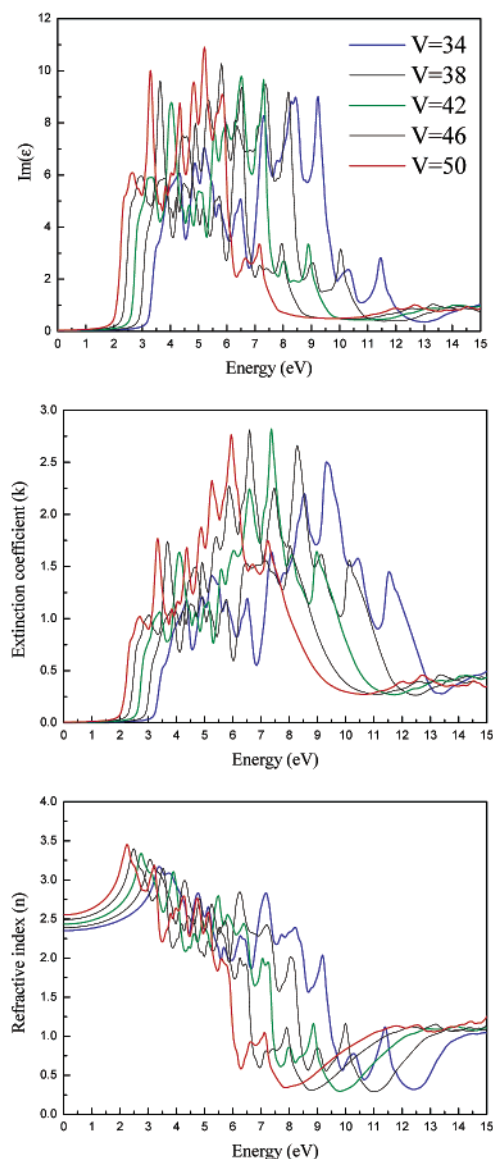


Figure 5. Calculated optical properties of a hypothetical CdI₂ structure¹⁸ of TiO₂ as a function of isotropic change in the volume formula unit: the isotropic imaginary part ϵ_2 of the dielectric function, the extinction coefficient k , and the refractive index n .

unit expected for this layered TiO₂ phase¹⁸ is 39.50 Å³. We varied the volume/formula unit of this layered phase in two different ways: (a) increase the interlayer distance while keeping fixed the structure of each TiO₂ layer (“anisotropic” volume increase); (b) increase the interlayer distance as well as the Ti–O bond length of each TiO₂ layer simultaneously

- (18) Soulard, C.; Rocquefelte, X.; Jobic, S.; Dai, D.; Koo, H.-J.; Whangbo, M.-H. *J. Solid State Chem.* **2003**, *175*, 353.
- (19) Hyde, B. G.; Andersson, S. *Inorganic Crystal Structures*; John Wiley & Sons: New York, 1989.
- (20) Grey, I. E.; Li, C.; Madsen, I. C.; Braunshausen, G. *Mater. Res. Bull.* **1988**, *23*, 743.
- (21) Gonschorek, W. Z. *Kristallogr.* **1982**, *160*, 187.
- (22) Baur, W. H. *Acta Crystallogr.* **1961**, *14*, 214.
- (23) Horn, M.; Schwerdtfeger, C. F.; Meagher, E. P. *Z. Kristallogr.* **1972**, *136*, 273.
- (24) Akimoto, J.; Gotoh, Y.; Oosawa, Y.; Nonose, N.; Kumagai, T.; Aoki, K.; Takei, H. *J. Solid State Chem.* **1994**, *113*, 27.
- (25) Feist, T. P.; Davies, P. K. *J. Solid State Chem.* **1992**, *101*, 275.
- (26) Sasaki, T.; Watanabe, M.; Fujiki, Y. *Acta Crystallogr. B* **1993**, *49*, 838.

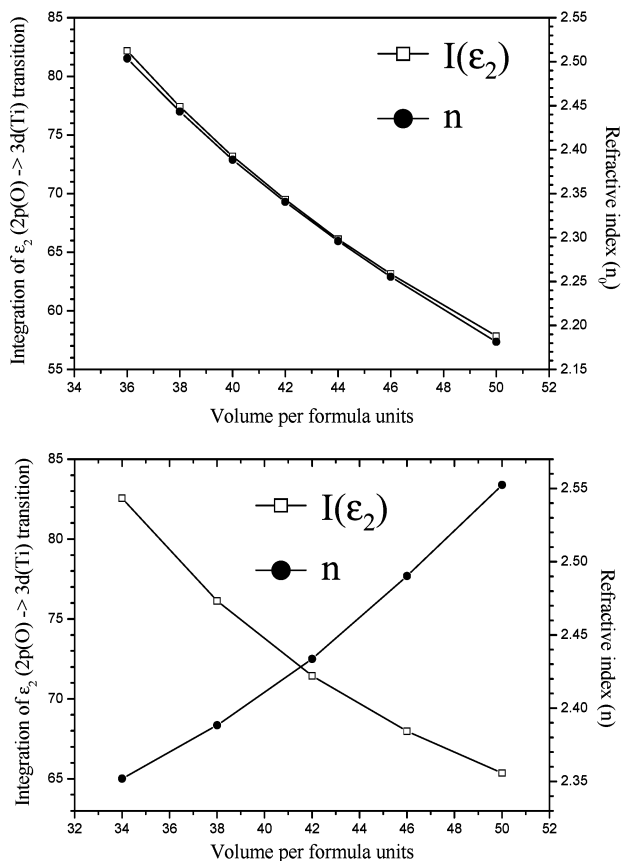


Figure 6. Normalized transition intensities $I(\epsilon_2)$ and refractive indices n_0 calculated for the CdI_2 phase of TiO_2 as a function of the anisotropic (top) and isotropic (bottom) change in the volume/formula unit.

(“isotropic” volume increase). In the case of “anisotropic” volume change (Figure 4), there is no variation in the optical gap because the electronic structure of an individual TiO_2 layer is not modified. Both n and $I(\epsilon_2)$ are calculated to decrease with increasing the volume/formula unit (top of Figure 6). (For example, the calculated refractive indices are 2.40, 2.18, and 1.70 for the volumes/formula unit of 39.50, 50, and 100 \AA^3 , respectively, which should be compared with 2.34, 2.06, and 1.53 calculated from the GD equation, respectively, Figure 2.) In the case of the “isotropic” volume change, however, the refractive index increases with increasing the volume/formula unit although the transition intensity $I(\epsilon_2)$ shows the opposite trend (bottom of Figure 6). In this case, the Ti–O bond length increases with increasing the volume/formula unit, which weakens the covalency of the

Ti–O bond and hence reduces the optical gap (Figure 5). Consequently, the $k(\omega)/\omega$ value becomes larger in the low-energy region, and the decrease in the optical gap exerts a greater effect on the refractive index than does that in the transition intensity.

Thus, our study shows why the GD equation works. In closely related compounds, the electronic structures are similar because the local chemical bonding features are the same so that their optical gaps do not vary very much. Therefore, the refractive index depends largely on the integrated transition intensity $I(\epsilon_2)$. As a consequence, the refractive index should decrease with increasing the volume/formula unit, hence with decreasing ρ_e or ρ_m .

In terms of absorption strength, Figures 4 and 5 show that the extinction coefficient k varies in the same way as does ϵ_2 . The anisotropic volume increase (Figure 4) induces only a continuous decrease of the intensity in the whole spectrum region, while the isotropic volume increase (Figure 5) leads mainly to a shift toward the lower energies and a contraction of the spectrum.

Concluding Remarks and Perspectives

The refractive index of a material is related to its ability to absorb the incident light in all energy range. The higher the integrated absorption intensity $I(\epsilon_2)$, the higher the refractive index is expected. The electronic origin of the GD equation is that the product $I(\epsilon_2)V$ is nearly constant. The compactness of the material, i.e., the concentration of chromophors or excitable electrons, plays a decisive role in determining the refractive index n . This finding points to the possibility of controlling the n value without changing the optical gap and with a homogeneous decrease of the extinction coefficient. For example, to decrease n , one might imagine separating building blocks. However, building blocks cannot be infinitely separated by void without losing the cohesion of the solid. Therefore, to obtain new UV blockers, it would be interesting to seek hybrid materials in which a component of desired chromophors is combined with another component of no chromophors.

Acknowledgment. Work at North Carolina State University was supported by the Office of Basic Energy Sciences, Division of Materials Sciences, U.S. Department of Energy, under Grant DE-FG02-86ER45259.

IC035383R